Stanford EE267: Virtual Reality
Course Report
Advanced Anaglyph Rendering Algorithm

Hayato Ikoma and Alexa Siu
Instructors: Gordon Wetzstein and Robert Konrad
e-mail: hikoma@stanford.edu, alexasiu@stanford.edu

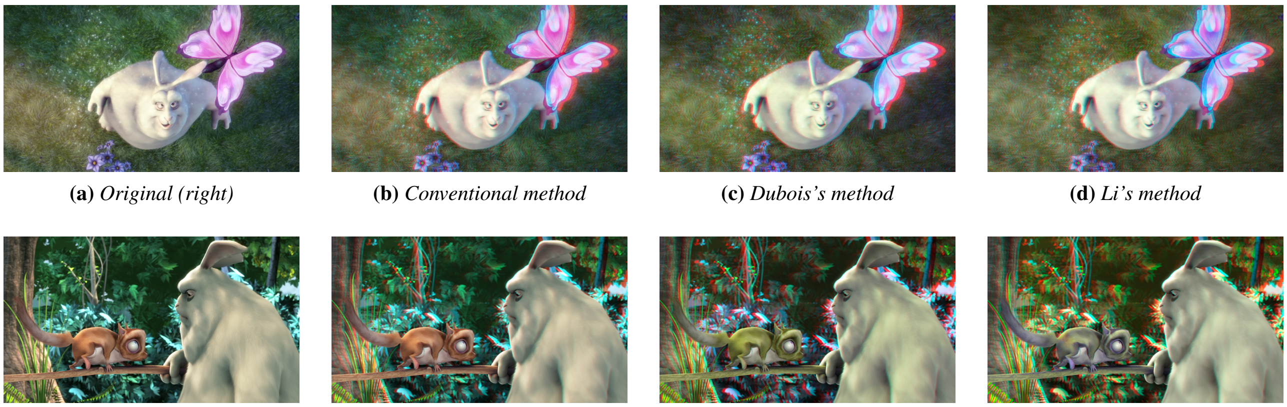

(a) *Original (right)* **(b)** *Conventional method* **(c)** *Dubois's method* **(d)** *Li's method*

(e) *Original (right)* **(f)** *Conventional method* **(g)** *Dubois's method* **(h)** *Li's method*

Figure 1: *Anaglyph images with three different methods.*

Abstract

Anaglyph rendering is the most inexpensive way to create a 3D effect. This method only requires a pair of red-cyan filter glasses, which blocks red light for a right eye and blue and green light for a left eye. This allows us to physically decompose a pair of left-and-right-eye images superimposed on a single monitor. Although this simple setup provides a 3D effect, it has disadvantages such as color distortion, retinal rivalry and ghosting effect. In this final project, among advanced anaglyph rendering algorithms, we reimplemented the algorithm introduced in [Li et al. 2013]. This method produced anaglyph images with suppressed retinal rivalry and ghosting effect but severely distorted red-like colors. To address this problem, we explored a way to improve color perception by a post processing step. We report a clue to recover such distorted color by encouraging our brain to recognize red-like color on selected regions with a left eye.

1 Introduction

Three dimensional (3D) displays are becoming popular consumer technologies. They mainly rely on the projection of two respective images to the right and left eyes. For example, some movie projectors superpose stereoscopic images on the same screen with orthogonal polarization states so that viewers wearing polarization glasses see different images with different eyes. Head-mounted displays exploit lenses with a near-eye display to directly display separate images to each eye. At the expense of their high-quality 3D effect, however, they require specialized hardware. Among such 3D technologies, anaglyph is the most inexpensive way for the projection of two different images. This method only requires a conventional display or even printed images, and corresponding 3-D anaglyph glasses. To render the anaglyph image, two stereoscopic images are combined into a single image using a complimentary color coding technique. The left stereoscopic image is stored in the red channel of the final image while the right stereoscopic image is stored in the green and blue channels. The red-cyan glasses wore by the viewer ideally only permit transmission of the correct image to each eye.

Although this simple setup provides a 3D effect, it lacks color preservation for both eyes due to the color filters. This lack is the main disadvantage of anaglyph rendering among others including retinal rivalry and ghosting effect. Retinal rivalry occurs when the anaglyph image cannot be properly fused by the brain. In this case, the image could appear to be alternating in colors. Ghosting or crosstalk occurs when an image intended solely to one eye is captured by the other eye. Ghosting reduces the image's visual quality by impeding image fusion and may also cause visual discomfort.

2 Related work

To address these problems, several algorithms have been developed for generating superior anaglyph images. In 2001, Dubois developed a least square method to minimize the color discrepancy between original stereoscopic images and anaglyph images in the CIE XYZ color space [Dubois 2001]. This XYZ anaglyph method significantly improved the color distortion and has been considered to be the state-of-the art method until recently. Following this work, McAllister et al. performed the minimization of Euclidian distance in the CIE $L^*a^*b^*$ space, which produced better color perception due to the perceptual linearity in CIE $L^*a^*b^*$ space [McAllister et al. 2010]. However, this $L^*a^*b^*$ anaglyph method is computationally expensive because it solves an iterative optimization problem on each pixel. To further improve color perception, Li et al. proposed a method to minimize the color discrepancy in HSL color space [Li et al. 2013]. In addition to its superior performance, their method significantly reduced the computational cost by finding an approximated closed-form solution of the minimizer. Similarly, this type of color-retaining algorithm has been developed for a projector in which color primaries are customized [Kauvar et al. 2015].

Most of the research around anaglyph rendering has focused on optimizing the production stage to increase color fidelity and reduce ghosting and retinal rivalry [Krupev and Popova 2008]. Krupev et al. proposed a post-production algorithm, for reducing ghosting effect by selectively reducing the R and G channels' intensity when above a certain threshold. Inair et al. explored color component blurring of anaglyph images to reduce conflicting depth cues and relief the convergence and accommodation conflict. They found blurring of the red and blue channels provided best results in increasing visual quality without compromising 3D perception. On the other hand, defocusing of the green channel proved to be destructive [Ideses and Yaroslavsky 2005].

In this final project, we re-implemented the state-of-the-art anaglyph rendering algorithm developed in [Li et al. 2013] and compared its performance on a freely-available stereoscopic computer animation movie. As we describe in detail in the following section, Li's algorithm produced the best 3D perception among the compared methods but significantly distorted color in regions with predominantly red-like colors. To achieve greater chrominance accuracy, we explored a post-processing method to encourage our brain to recognize red color from the left-eye image but not from right-eye image.

3 Methods

3.1 Display Device Measurements

As described in [Dubois 2001], anaglyph rendering should be optimized for specific anaglyph glasses and displays. Their spectral characteristics determine the conversion from device specific RGB to XYZ color space. To find this proper conversion, we measured the emission spectra of display primaries from a MacBook Pro (2015) Retina display and the transmission spectra of standard cardboard red-cyan anaglyph glasses with a calibrated Ocean Optics USB4000 spectrometer.

For the measurements of the emission spectra of the RGB primaries, we recorded the readings from the spectrometer coupled with an optical fiber placed in front of the monitor. For each measurement, fullscreen uniform red, green and blue images were displayed to have pure spectra, respectively. The measured spectra are plotted in Figure 4a. In addition, the measurements were also used to confirm the gamma value of the MacBook monitor to be 2.2.

Similarly, the transmission spectra for each color filter in the anaglyph 3-D glasses were also measured using a halogen lamp as a white light source. Figure 3 shows the experimental setup with the halogen light, and Figure 4b shows the resulting transmission spectra for both red and cyan filters.

3.2 Conversion from sRGB to *L*a*b** color space

sRGB is the most widely used color space for displaying digital color images. Since the images we will be using are in the sRGB color space, the first step in the conversion to *L*a*b** space is to convert from sRGB to RGB. This conversion from device-dependent coordinates to RGB is known as gamma correction [Dubois 2009]. The conversion can be described by a power law function,

$$g(x) := \begin{cases} \frac{x}{12.92} & \text{if } x < 0.04045 \\ (\frac{x+0.055}{1.055})^{2.4} & \text{otherwise} \end{cases}$$

where $x \in [0,\, 1]$. After gamma correction, the stereo pair images are converted to *L*a*b** space. This step involves converting from RGB values $(R_\mathrm{l}, G_\mathrm{l}, B_\mathrm{l}, R_\mathrm{r}, G_\mathrm{r}, B_\mathrm{r})$ to the CIE XYZ color space $(X_\mathrm{l}, Y_\mathrm{l}, Z_\mathrm{l}, X_\mathrm{r}, Y_\mathrm{r}, Z_\mathrm{r})$ based on the following linear equations:

$$\begin{bmatrix} X_\mathrm{l} \\ Y_\mathrm{l} \\ Z_\mathrm{l} \end{bmatrix} = C \begin{bmatrix} R_\mathrm{l} \\ G_\mathrm{l} \\ B_\mathrm{l} \end{bmatrix} \quad \text{and} \quad \begin{bmatrix} X_\mathrm{r} \\ Y_\mathrm{r} \\ Z_\mathrm{r} \end{bmatrix} = C \begin{bmatrix} R_\mathrm{r} \\ G_\mathrm{r} \\ B_\mathrm{r} \end{bmatrix}$$

where C is a 3×3 real matrix. The display's measured emission spectra from Section 3.1 and color matching functions are then used to compute the linear transformation matrix, C [Dubois 2001]. The matrix corresponding to our display was computed to be

$$C = \begin{bmatrix} 0.339912 & 0.383697 & 0.0835086 \\ 0.180096 & 0.758434 & 0.0614702 \\ 0.00948206 & 0.0726193 & 0.375276 \end{bmatrix}. \tag{1}$$

While the matrix C allows conversion from RGB to CIE XYZ color space, it does not take into account the filtering from the glasses. Two additional matrices need to be calculated, one for each filter which converts from RGB to CIE XYZ color space and models the filtering. For this computation, the anaglyph's transmission spectrum for the red and blue filters were used. The matrix corresponding to the right eye (cyan filter) is

$$C_\mathrm{r} = \begin{bmatrix} 0.0269114 & 0.284459 & 0.0357779 \\ 0.0194866 & 0.891309 & 0.0892045 \\ 0.00353967 & 0.0969519 & 0.15132 \end{bmatrix}. \tag{2}$$

The matrix corresponding to the left eye (red filter) is

$$C_\mathrm{l} = \begin{bmatrix} 1.69841 & 0.232961 & 0.0231218 \\ 0.832751 & 0.155349 & 0.0119002 \\ 0.000713731 & 0.000918523 & 0.00399096 \end{bmatrix}. \tag{3}$$

After conversion to the XYZ color space, the values are finally converted into CIE *L*a*b** color space values $(L_\mathrm{l}, a_\mathrm{l}, b_\mathrm{l}, L_\mathrm{r}, a_\mathrm{r}, b_\mathrm{r})$ [Dubois 2009]. This conversion is performed based on the following nonlinear transform for $i \in \{\mathrm{r}, \mathrm{l}\}$:

$$\begin{aligned} L_i &= 116\, f(Y_i/Y_\mathrm{w}) - 16 \\ a_i &= 500\, (f(X_i/X_\mathrm{w}) - f(Y_i/Y_\mathrm{w})) \\ b_i &= 200\, (f(Y_i/Y_\mathrm{w}) - f(Z_i/Z_\mathrm{w})) \\ &\text{where } f(t) := \begin{cases} t^{1/3} & \text{if } t \le 0.008856 \\ 7.787t + 0.1379 & \text{otherwise.} \end{cases} \end{aligned}$$

3.3 Li's method

In this section, we describe Li's algorithm for anaglyph rendering. Li's method starts with processing of the right stereoscopic image followed by processing of the left image. Based on the computed stereo pair *L*a*b** values $(L_\mathrm{l}, a_\mathrm{l}, b_\mathrm{l}, L_\mathrm{r}, a_\mathrm{r}, b_\mathrm{r})$, the goal is to compute $(L_\mathrm{Al}, a_\mathrm{Al}, b_\mathrm{Al}, L_\mathrm{Ar}, a_\mathrm{Ar}, b_\mathrm{Ar})$ of the perceived anaglyph such that they match the lightness, hue, and saturation of $(L_\mathrm{l}, a_\mathrm{l}, b_\mathrm{l}, L_\mathrm{r}, a_\mathrm{r}, b_\mathrm{r})$. In the end, the chosen $(L_\mathrm{Al}, a_\mathrm{Al}, b_\mathrm{Al})$ should be representable by a single red RGB value (R_Al) corresponding to the left image and the chosen $(L_\mathrm{Ar}, a_\mathrm{Ar}, b_\mathrm{Ar})$ should be representable by $(G_\mathrm{Ar}, B_\mathrm{Ar})$ corresponding to the right image.

3.3.1 Right image processing

To better minimize perceptual color appearance attributes, the right image is first converted into HSL color space for direct manipulation of lightness, hue, and saturation. Hue (H_r) and saturation (S_r)

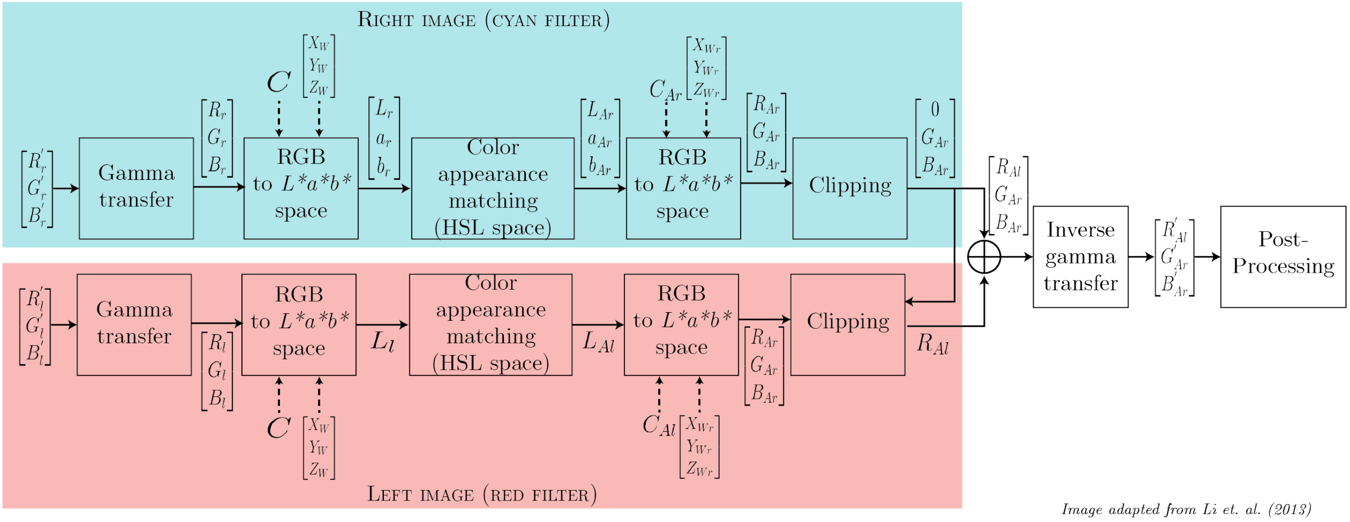

Figure 2: *Summary of the anaglyph rendering pipeline*

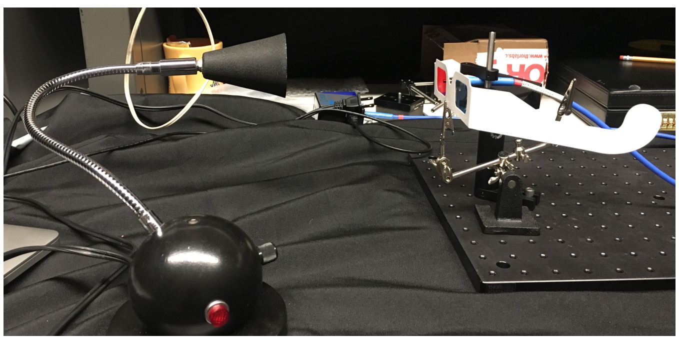

Figure 3: *Experimental setup for measuring the transmission spectra of the anaglyph glasses' red and cyan filters.*

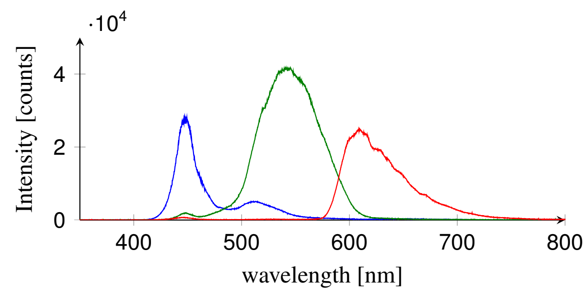

(a) *Display primaries of the Macbook Pro (2015) retina display*

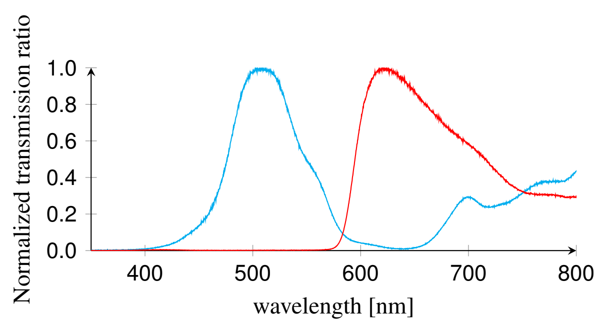

(b) *Transmission spectra of the anaglyph filters*

Figure 4: *Spectroscopy measurements used to compute the linear transformation matrices relating RGB to XYZ.*

can be computed from $a*$ and $b*$ by

$$H_{\mathrm{r}} = \frac{180}{\pi}(\tan^{-1}(\frac{b_{\mathrm{r}}}{a_{\mathrm{r}}}) + \pi u(-a_{\mathrm{r}}))$$
$$S_{\mathrm{r}} = \sqrt{a_{\mathrm{r}}^2 + b_{\mathrm{r}}^2}$$

where $u(\cdot)$ is the unit step function. Based on these H_{r} and S_{r} values, $(L_{\mathrm{Ar}}, a_{\mathrm{Ar}}, b_{\mathrm{Ar}})$ can be determined such that

1. the lightness, hue and saturation match those of $(L_{\mathrm{r}}, a_{\mathrm{r}}, b_{\mathrm{r}})$,
2. in the RGB color space, they can be represented by $(R_{\mathrm{Ar}} = 0, G_{\mathrm{Ar}}, B_{\mathrm{Ar}})$.

For the most part, the image lightness remains unchanged ($L_{\mathrm{Ar}} = L_{\mathrm{r}}$); however, for red-like colors, the lightness is reduced by a maximum of 40%. This was empirically determined to improve the image's chrominance accuracy of red-like colors at the expense of retinal rivalry and lightness preservation.

To ensure the second condition is met, the surface of 256×256 RGB values mapped by $(R_{\mathrm{Ar}} = 0, G_{\mathrm{Ar}}, B_{\mathrm{Ar}})$ is approximated by,

$$\begin{cases} b_{\mathrm{Ar}} = k\, a_{\mathrm{Ar}} & \text{if } a_{\mathrm{r}} > 0 \\ (a_{\mathrm{Ar}} - a_{\mathrm{c}})^2 - (b_{\mathrm{Ar}} - b_{\mathrm{c}})^2 = a_{\mathrm{c}}^2 + b_{\mathrm{c}}^2 & \text{otherwise} \end{cases}$$

where $k = -0.7273$, $a_c = 125$, and $b_c = 172$. Values are projected onto this blue-green region and determined by

$$\sqrt{a_{Ar}^2 + b_{Ar}^2} = \begin{cases} S_{\mathrm{r}} \frac{H_{\mathrm{r}} - H_{\mathrm{RED}}}{T} & \text{if } |H_{\mathrm{r}} - H_{\mathrm{RED}}| \leq T \\ S_{\mathrm{r}} \frac{H_{\mathrm{r}} - H_{\mathrm{CYAN}}}{T} & \text{if } |H_{\mathrm{r}} - H_{\mathrm{CYAN}}| \leq T \\ S_{\mathrm{r}} & \text{otherwise.} \end{cases}$$

The details of this approximation and the projection is described in the original paper [Li et al. 2013].

The last step in processing the right image is to convert the resulting $(L_{\mathrm{Ar}}, a_{\mathrm{Ar}}, b_{\mathrm{Ar}})$ values back to the device RGB color space using a similar procedure as in 3.2 and retaining only the green and blue channels ($R_{\mathrm{Ar}} = 0, G_{\mathrm{Ar}}, B_{\mathrm{Ar}}$). For the CIE XYZ to RGB conversion, the linear conversion matrix found in Equation (2) should be used instead of Equation (1).

3.3.2 Left image processing

The left anaglyph image is produced in a way to suppress retinal rivalry. In anaglyph rendering, retinal rivalry is known to be mainly caused by the difference in lightness between left and right images. Therefore, the left image is rendered to match the lightness to the right anaglyph image. In typical stereoscopic images, the lightness at the same physical position are the same in the original left and right images. Since the right anaglyph image mostly preserves the lightness from the original right image, the left anaglyph rendering is boiled down to represent an image only with red channel while preserving the original lightness. While this processing suppresses retinal rivalry, the ghosting effect appears due to the luminance leakage. As can be seen in C_{l} and C_{r}, the leakage is negligible in the right image but significant in the left image. Therefore, subtractive ghosting reduction is commonly performed in the conversion to RGB color space.

From the anaglyph image, the left eye perceives the lightness

$$\begin{aligned} L_{\mathrm{Al}} = 116\, f((0.832751\, R_{\mathrm{Al}} \\ + 0.155349\, G_{\mathrm{Ar}} + 0.0119002\, B_{\mathrm{Ar}})/Y_{\mathrm{wl}}) - 16. \end{aligned}$$

The green and blue channels in the anaglyph image $G_{\mathrm{Ar}}, B_{\mathrm{Ar}}$ are computed in the right image processing step so that the red channel can be computed by

$$R_{\mathrm{Al}} = \frac{\max(Y_{\mathrm{Al}} - 0.155349\, G_{\mathrm{Ar}} -\ 0.0119002 B_{\mathrm{Ar}},\ 0)}{0.832751}$$

where $Y_{\mathrm{Al}} = Y_{\mathrm{Wl}}\, f^{-1}((L_{\mathrm{Al}} + 16)/116)$. The inverse of the function $f(\cdot)$ is easily found to be

$$f^{-1}(t) = \begin{cases} t^3 & \text{if } t \geq 0.2069 \\ 0.1284(t - 0.1379) & \text{otherwise.} \end{cases}$$

3.4 Results from Li's method

We implemented Li's algorithm described above in Julia language. We compared our implementation and Li's MATLAB implementation in terms of its runtime. For this comparison, we used a single core of Intel Core i7-4790 CPU (3.60GHz) and processed a pair of 1080×1920 images. In this comparison, Li's implementation took 1.74 seconds while our implementation took 0.74 seconds. Furthermore, our implementation can process multiple images in parallel, which is advantageous to produce an anaglyph video.

To demonstrate its performance, we processed the Big Buck Bunny movie freely available online (https://peach.blender.org/). Selected frames of the resulting anaglyph video are shown in Figure 1. For comparison, anaglyph images produced with the conventional method and Dubois's method available on their website are also shown. Given time constraints, we did not carry out a formal user study. However, subjective feedback from peers was generally positive. Most negative feedback came from inaccuracies in the anaglyph images' color when compared to the original stereoscopic images.

While the results from the conventional method induced significant retinal rivalry, Li's method produced anaglyph images that have better 3D perception due to the suppression of retinal rivalry. However, the regions containing red components such as pink and brown colors significantly suffered from color distortion. The quality of visual color reproduction highly depends on image fusion by the brain's visual cortex. The human visual system has higher sensitivity to green hues [Ideses and Yaroslavsky 2005]. Therefore, we hypothesize that in regions of predominantly red-like colors, much crosstalk from the right eye image (which has red filtered out) is occurring.

4 Color enhancement post-processing

4.1 Algorithm

To retain chrominance accuracy in regions where red color is dominant, we explored a combination of selective color intensity reduction and color defocusing on the final rendered anaglyph. The algorithm first increases the red channel's intensity and decreases the green and blue channels' intensity. Next, the green and blue channels are filtered with a 2-D Gaussian smoothing kernel. By applying these two operations, the goal is to alleviate retinal rivalry and decrease any crosstalk between images. This decreases the high-frequency in the green and blue channels so the images can be fused more smoothly. It also relies on the monovision effect to preserve the image's details despite the applied blurring. If the post-processed anaglyph image is seen with only the cyan filter, all red color regions should therefore appear blurred and darker than the image seen through the left eye only. The post-processing algorithm is summarized in Algorithm 1.

Algorithm 1 Anaglyph post-processing

```
for All pixels in anaglyph image do
    rgb = current pixel RGB vector
    rgb_r = current pixel RGB vector in right stereo
    rgbRed = current pixel RGB storing high red regions
    if rgb_r[1]/rgb_r[2] ≥ threshold
          and rgb_r[1]/rgb_r[3] ≥ threshold then
        Compute s = sqrt( rgb_r[1]^2 / (rgb_r[2]^2 + rgb_r[3]^2) )
        rgbRed[1] = rgb[1] * s
        rgbRed[2] = rgb[2]/s
        rgbRed[3] = rgb[3]/s
        filteredImg[current pixel] = rgbRed
    end if
end for
Only keep the largest cluster of color pixels in filteredImg
Blur green and blue channel of filteredImg with Gaussian filter
of variance 2.0
Replace RGB pixels in the original anaglyph with corresponding
pixels from fitleredImg
```

4.2 Results from post-processing

Figure 6 shows an anaglyph image rendered with Li's method. This image has primarily red-like colors but after anaglyph rendering appears more purple. Figure 5 shows the results of applying our post-processing algorithm. The threshold used for selecting the dominant red-regions in this image was 2.0. This value was tuned subjectively for this image. The method works well in achieving greater chrominance accuracy in certain regions. We highlight this difference in the cropped section of the image on the right. For other regions, however, the post-processing method increases the ghosting effect and the image loses some of its 3-D quality. Another disadvantage is that while we were able to tune the algorithm's parameters to work well in an image-by-image basis, we were not able

Figure 5: *Anaglyph image after color enhancement post-processing. [3DChina, http://www.china3-d.com/3dclub/]*

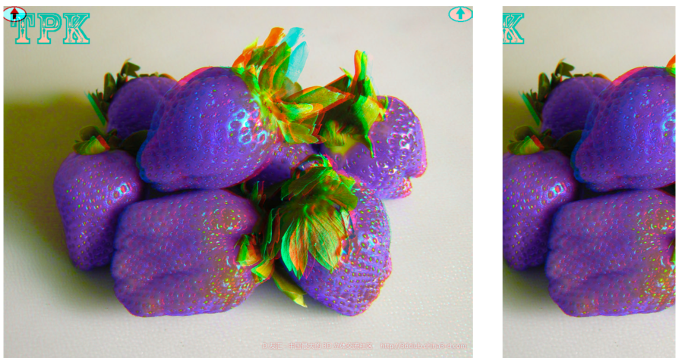

Figure 6: *Image after anaglyph rendering algorithm. [3DChina, http://www.china3-d.com/3dclub/]*

to achieve a universally sound and systematic way of applying the post-processing.

5 Discussion & Conclusion

Anaglyph rendering is still an unsolved problem. Since anaglyph glasses inherently discard and distort some part of light, there is no way to generate color-undistorted anaglyph images. As Dubois's work and its follow-up works have demonstrated, color appearance matching is a crucial step to minimize color distortion originated in anaglyph rendering. However, we observed that these methods sacrifice red perception.

To address this problem, we explored a way to retain such red-like colors through a post-processing algorithm. Our algorithm is not a universal method, but we demonstrated that the combination of monovision and lightness discrepancy is a key to consistently let our brain recognize color from the left eye on red-dominant regions. Wavelet analysis on each color channel and region-dependent blurring may lead to develop a universal post processing algorithm.

References

Dubois, E. 2001. A projection method to generate anaglyph stereo images. In *Proceedings of ICASSP 2001*, vol. 3, 1661–1664.

Dubois, E. 2009. *The Structure and Properties of Color Spaces and the Representation of Color Images*. Morgan & Claypool.

Ideses, I., and Yaroslavsky, L. 2005. Three methods that improve the visual quality of colour anaglyphs. *Journal of Optics A: Pure and Applied Optics 7*, 12, 755.

Kauvar, I., Yang, S., Shi, L., McDowall, I., and Wetzstein, G. 2015. Adaptive Color Display via Perceptually-driven Factored Spectral Projection. *ACM Transactions on Graphics*.

Krupev, A. A., and Popova, A. A. 2008. Ghosting reduction and estimation in anaglyph stereoscopic images. In *2008 IEEE International Symposium on Signal Processing and Information Technology*, 375–379.

Li, S., Ma, L., and Ngan, K. N. 2013. Anaglyph image generation by matching color appearance attributes. *Signal Processing: Image Communication 28*, 6, 597–607.

McAllister, D. F., Zhou, Y., and Sullivan, S. 2010. Methods for computing color anaglyphs. *Proceedings of SPIE 7524*, 75240S–75240S–12.

Patana, E., Safonov, I., and Rychagov, M. 2013. *Transactions on Computational Science XIX: Special Issue on Computer Graphics*. Springer Berlin Heidelberg, Berlin, Heidelberg, ch. Adaptive Generation of Color Anaglyph, 33–47.